The Astronomical Journal, 125:3185–3195, 2003 June

SEARCHING FOR PLANETS IN THE HYADES. IV. DIFFERENTIAL ABUNDANCE ANALYSIS OF HYADES DWARFS[1]

Diane B. Paulson and Christopher Sneden
Department of Astronomy, University of Texas, Austin, TX 78712; apodis@astro.as.utexas.edu, chris@verdi.as.utexas.edu

and

William D. Cochran
McDonald Observatory, University of Texas, Austin, TX 78712; wdc@astro.as.utexas.edu
Received 2003 February 11; accepted 2003 March 5

ABSTRACT

We present a differential abundance analysis of Hyades F–K dwarfs in search for evidence of stellar enrichment from accreted hydrogen-deficient disk material. Metallicities and relative abundance ratios of several species have been determined. We derive a cluster mean [Fe/H] = 0.13 ± 0.01. Two stars show abundances ~0.2 dex larger than the cluster mean. In addition, one star, which was added by a recent study as a cluster member, shows significantly lower abundances than the cluster mean. These three stars have questionable membership characteristics. The remaining stars in the survey have an rms of 0.04 dex in the differential [Fe/H] values. The Hyades cluster members have apparently not been significantly chemically enriched. The abundance ratios of Si, Ti, Na, Mg, Ca, and Zn with respect to Fe are in their solar proportions.

Key words: open clusters and associations: individual (Hyades) — stars: abundances

1. INTRODUCTION

The proposition that extrasolar planet host stars tend to be metalrich has implications for the planet formation community. This fact, as shown by, e.g., Gonzalez (1997, 1998), Laughlin & Adams (1997), and Jeffery, Bailey, & Chambers (1997), although interesting, has not yet been given a single, universally accepted theoretical explanation. Two possibilities are reviewed well by Murray & Chaboyer (2002) and Smith, Cunha, & Lazzaro (2001)—either planets form preferentially around stars that are intrinsically richer in heavy elements, or the overabundance of metals is due to hydrogen-deficient protoplanetary debris enriching the stellar photosphere. Only stars that have shallow convection regions will show metal enrichment due to accretion; when a star has a large convective region, the additional metals will be diluted beyond detection. For F stars and earlier, enrichment can occur during the early life as a main-sequence star; however, for G stars, enrichment is thought to occur only if the accretion has taken place after the first 10 Myr of pre–main-sequence evolution. At this time the convective region has decreased in size (Murray & Chaboyer 2002; Pinsonneault, DePoy, & Coffee 2001; Laughlin & Adams 1997). Latertype stars should show no detectable enhancement, even if large amounts of material are accreted.

Current searches for planets include stars with vastly different chemical and formation histories. One good way to test the enrichment theory is by observing a star cluster, whose members were presumably formed from homogeneous material. The key is to look for star-to-star differences in heavyelement content. Stars showing higher amounts of metals would have had to be enriched in some way, notably from H-deficient material being accreted onto the stellar atmosphere. Similar programs have utilized this concept of eliminating the initial composition variable by performing a differential abundance analysis of binary stars (Laws & Gonzalez 2001; Gratton et al. 2001). Recently, a program similar to this one has been undertaken by Fulbright (2002).

Abundances of Hyades stars have been determined by several groups over the past few decades. These studies have provided increasingly more accurate abundances, as atomic data have improved and as stellar atmosphere models have come to more closely approximate physical reality. Varenne & Monier (1999) review the abundance studies of the Hyades from Conti, Wallerstein, & Wing (1965) through their own work. The measurement of heavy elements has been studied for A-F stars, but a detailed analysis in the lower mass dwarfs is lacking. In addition, many of these studies only include one or two dozen stars. Conti et al. studied various elements in 10 Hyades stars. They were also interested in looking for star-to-star differences to determine if the protocluster nebula was homogeneous. This survey provided the first evidence that Li in the Hyades is not uniform, while the abundances of several other elements were. To within their stated error bars, Conti et al. determined that the abundance of Hyades members is constant for all elements but Li. Later, chemical composition studies (excluding studies of only Fe and/or Li, which are more numerous) were completed for A–F stars by Boesgaard, Heacox, & Conti (1977), Burkhart & Coupry (1989), Friel & Boesgaard (1990), García López et al. (1993), Takeda & Sadakane (1997), Hui-Bon-Hoa & Alecian (1998), Burkhart & Coupry (2000), and Takeda et al. (1998). For lower mass stars, heavyelement abundance determinations were only completed by (again excluding studies of only Fe and/or Li) Conti et al. (1965), King & Hiltgen (1996), and Boesgaard et al. (1977). Further papers instrumental to the metallicity determination of the Hyades cluster are Boss (1989), Branch, Lambert, & Tomkin (1980), Boesgaard & Budge (1988), Cayrel, Cayrel de Strobel, & Campbell (1985), and Chaffee, Carbon, & Strom (1971).

[1] Some data presented herein were obtained at the W. M. Keck Observatory, which is operated as a scientific partnership among the California Institute of Technology, the University of California, and the National Aeronautics and Space Administration. The Observatory was made possible by the generous financial support of the W. M. Keck Foundation.

Pinsonneault et al. (2001) estimated the amount of Fe that must be accreted onto the stellar photosphere in order to enrich the measured [Fe/H] of a solar-type star appreciably. They find that a quantity of 10 $M_{\oplus}$ of Fe (a rough upper limit to the Fe core of Jupiter) would increase the [Fe/H] of a solar-type star by 0.09 dex. Within the errors of stellar abundance analysis and atomic data, variations of this magnitude within the cluster are detectable through a differential abundance analysis.

In this paper, one in a series exploring planets and planet formation in the Hyades cluster (e.g., Cochran, Hatzes, & Paulson 2002; Paulson et al. 2002, 2003), we present abundance determinations for Fe, Si, Ti, Ca, Na, Mg, and Zn (as well as differential measurements for each of these elements) for a large sample of Hyades members over a wide effective temperature range in search of evidence of stellar enrichment.

2. OBSERVATIONS

2.1. *Sample*

The planet search program, undertaken with the Keck I HIRES (Vogt et al. 1994), contains 98 F-M dwarfs (Cochran et al. 2002). The present chemical composition analysis, which makes use of these spectra, unfortunately does not include all 98 stars. The M dwarfs and a few late K dwarfs ($B-V$ cutoff of 1.0) were not analyzed because of the crowded spectra, inability to accurately place the continuum, and the poorer S/N achieved for these stars. At the beginning of the survey, we selected only stars that were thought to have no stellar companions. In a few cases, we did select wide binaries that were sufficiently separated in the sky that we would have no contamination in the spectra from the companion. However, since that time, four stars in the original sample are now known to have non–planetary-mass companions (vB 5, vB 52, vB 17 [Patience et al. 1998], and vB 88). The discovery of these stellar companions does not prevent us from detecting planets, nor should it affect the overall abundance determinations in this paper. Stars showing linear trends in radial velocity (perhaps additional unknown binaries) have therefore been included. Also included in this sample is one star, HD 14127, that has been monitored in the planet search program but which, we are now confident, is not a member. A second, HIP 13600, also may not be a member. These are discussed further in § 3.6. The final sample size for this abundance study is 55 stars.

2.2. *Spectra*

A full description of the observations can be found in Cochran et al. (2002). All spectra were obtained at the Keck I telescope from 1996 to 2002. We have used HIRES with resolving power ($R = \Delta\lambda/\lambda$) nominally at 60,000. The S/N of each spectrum is typically 100–200 per pixel (see examples in Fig. 1). The wavelength range of (3805–6188 Å) was chosen so that all I_2 absorption lines are included for radial velocity measurements and so that the Ca II H and K lines could be monitored for stellar activity. Unfortunately, this wavelength range excludes the spectral lines of many interesting elements (e.g., Li). The spectra used for abundance analysis are those taken as "template" spectra for use in the radial velocity program. Thus, these spectra are free of I_2 absorption. Observations of hot stars are unnecessary because of the extreme lack of moisture at the Mauna Kea site. Therefore, the telluric absorption will be very weak. All Keck spectra were reduced using standard IRAF[2] packages.

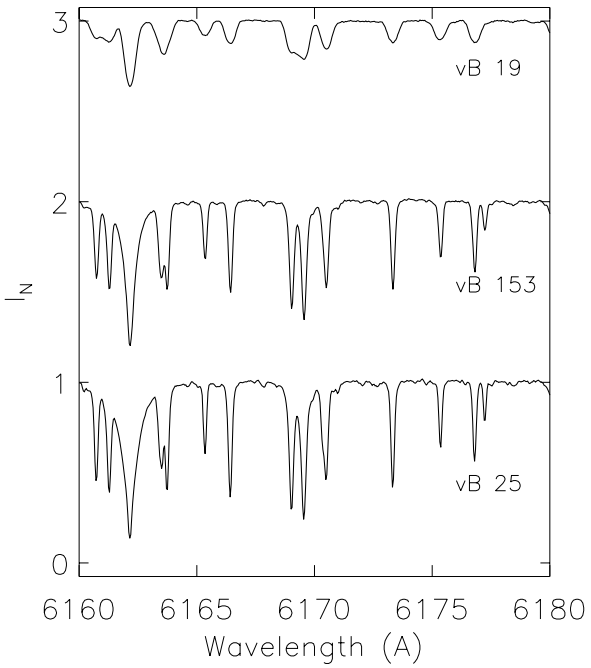

FIG. 1.—Example spectra from our survey. We show here how some lines become blended with increasing rotational velocity and increasing $T_{\rm eff}$. We have added 1 and 2 units, respectively, to the normalized intensity (I_N) of vB 153 and vB 19. Our warmest star is vB 19, our coolest star is vB 25, and vB 153 is our comparison star.

3. ABUNDANCE ANALYSIS

The abundance analysis makes use of the current version of the LTE line analysis code MOOG (Sneden 1973). The line list is compiled from three sources: Fe I and II *gf* values were derived internally (as described in § 3.2), and the remaining parameters were obtained from either R. E. Luck (2003, private communication) or Kurucz & Bell (1995). The final line list is given in Table 1, and the sources for excitation potential (χ) and oscillator strength (*gf* value) are listed as well. In deriving [Fe/H][3] and [X/Fe] values, solar values were derived from a solar spectrum (of Ceres) taken through HIRES. Originally, we adopted the values from Grevesse & Sauval (1998), but we found a difference of 0.14 dex between our derived $\log\epsilon(\mathrm{Fe})_{\odot}$[4] and that found by Grevesse & Sauval. The difference is primarily due to instrumental effects. Thus, in order to eliminate instrumental uncertainties, we used $\log\epsilon(\mathrm{Fe})_{\odot}$ as derived from our solar spectrum. The values of $\log\epsilon(\mathrm{X})_{\odot}$ were also in disagreement with Grevesse & Sauval, so again, we chose to use the values derived from our solar spectrum.

3.1. *Stellar Parameters*

We determined stellar parameters using the template spectra obtained from Keck HIRES. We normalized the

[2] IRAF is distributed by the National Optical Astronomy Observatory, which is operated by the Association of Universities for Research in Astronomy, Inc., under cooperative agreement with the National Science Foundation.

[3] $[A/B] = \log(A/B)_{*} - \log(A/B)_{\odot}$.

[4] Where $\log\epsilon(\mathrm{Fe})_{\odot} = n_{\mathrm{Fe}}/n_{\mathrm{H}} + 12.0$.

TABLE 1
Line List

Species	Wavelength	χ (eV)	$\log gf$	Reference
Na I.....	6154.226	2.100	−1.570	1
Na I.....	6160.747	2.100	−1.270	1
Mg I.....	5711.088	4.346	−1.833	2
Si I.....	5948.541	5.080	−1.230	1
Si I.....	6125.021	5.610	−1.513	1
Si I.....	6142.483	5.620	−1.540	1
Si I.....	6145.016	5.610	−1.479	1
Ca I	5260.387	2.521	−1.719	1
Ca I	6166.439	2.520	−1.142	1
Ca I	6169.042	2.520	−0.797	1
Ti I	5922.110	1.046	−1.410	1
Ti I	5937.811	1.066	−1.834	1
Ti I	5941.752	1.053	−1.454	1
Ti I	5953.162	1.887	−0.273	1
Ti I	5965.828	1.879	−0.353	1
Ti I	5978.543	1.873	−0.440	1
Ti I	6064.629	1.046	−1.888	1
Ti I	6126.217	1.066	−1.369	1
Fe I.....	5322.041	2.279	−2.840	2, 3
Fe I.....	5811.919	4.143	−2.430	2, 3
Fe I.....	5853.161	1.485	−5.280	2, 3
Fe I.....	5855.086	4.608	−1.600	2, 3
Fe I.....	5856.096	4.295	−1.640	2, 3
Fe I.....	5858.785	4.221	−2.260	2, 3
Fe I.....	5927.797	4.652	−1.090	2, 3
Fe I.....	5933.803	4.639	−2.230	2, 3
Fe I.....	5940.997	4.178	−2.150	2, 3
Fe I.....	5956.706	0.859	−4.605	2, 3
Fe I.....	5969.578	4.283	−2.730	2, 3
Fe I.....	6019.364	3.573	−3.360	2, 3
Fe I.....	6027.051	4.076	−1.090	2, 3
Fe I.....	6054.080	4.372	−2.310	2, 3
Fe I.....	6105.130	4.549	−2.050	2, 3
Fe I.....	6151.618	2.176	−3.290	2, 3
Fe I.....	6157.728	4.076	−1.110	2, 3
Fe I.....	6159.380	4.608	−1.970	2, 3
Fe I.....	6165.360	4.142	−1.470	2, 3
Fe I.....	6173.336	2.223	−2.880	2, 3
Fe II.....	4491.407	2.855	−2.490	2, 3
Fe II.....	4508.290	2.856	−2.310	2, 3
Fe II.....	4620.520	2.828	−3.230	2, 3
Fe II.....	5197.559	3.230	−2.250	2, 3
Fe II.....	5264.810	3.231	−3.150	2, 3
Fe II.....	5325.559	3.221	−3.170	2, 3
Fe II.....	5414.046	3.221	−3.620	2, 3
Fe II.....	5425.247	3.199	−3.210	2, 3
Fe II.....	6149.246	3.889	−2.720	2, 3
Zn I	4722.153	4.030	−0.338	2
Zn I	4810.528	4.078	−0.137	2

References.—(1) Provided by E. Luck (2003, private communication); compilation from various sources; (2) from Kurucz Atomic Line Database (Kurucz & Bell 1995); (3) $\log gf$ values derived from our solar spectrum and χ from Kurucz & Bell 1995.

continuum using IRAF. All equivalent widths (EWs) were measured by fitting a Gaussian to the observed line profiles, also using IRAF.

The stellar models used were interpolated[5] atmosphere models (with no convective overshoot) based on the 1995 version of ATLAS9 code (Castelli, Gratton, & Kurucz 1997). The relevant stellar parameters—effective temperature ($T_{\rm eff}$), gravity ($\log g$), and microturbulence (ξ)—were determined in the following manner. $T_{\rm eff}$ values were obtained by requiring that the Fe abundances of individual lines be independent of the excitation potential (χ). Microturbulence was determined by forcing Fe abundances from individual Fe I lines to be independent of line strength. Surface gravity was derived by requiring ionization equilibrium—the Fe abundance derived from Fe I lines must match that derived from Fe II lines. All stellar parameters are determined simultaneously, with the only requirement being that $\log g$ is confined to the range 4.2–4.7, a reasonable range given the known cluster distance. Derived stellar parameters are listed in Table 2. The method by which we determine stellar parameters also gives us the $\log \epsilon$(Fe) for each star. We thus list [Fe/H] for each star in Table 3.

In our abundance computations, we chose a van der Waals line damping parameter option with the Unsöld (1955) approximation. We also experimented with other damping enhancements recommended by Blackwell, Lynas-Gray, & Smith (1995) and Holweger (1971) to determine if one is significantly better for this set of data than the others. All three damping options were tested both by using the curve-of-growth analysis and by comparing the line shapes in a spectral region using a synthesis approach. We determined that neither of these enhancements to the Unsöld approximation yields a better fit to the lines chosen. The effect of damping was more apparent in the abundance analysis, where it was clear that the damping parameter affected the cooler stars more than the warmer stars (yielding slightly different abundances along the main sequence). In an absolute abundance analysis, the choice of different damping parameters does not seem to affect the final results. In an absolute abundance analysis, the comparison is made to the overall solar abundance, which changes only slightly with the different damping options (0.02 dex). The effect of damping on a differential analysis becomes slightly more pronounced. We compared the results of differential abundances of two stars and the Sun with varying damping parameters. The greatest difference was in vB 143 (compared to the standard vB 153), which showed changes of 0.06 dex between the Holweger and the Blackwell et al. suggested enhancements. The solar spectrum (also compared to vB 153) showed a difference of 0.04 dex, and vB 15 (compared to vB 153) showed 0.03 dex. There is no significant trend in these results with stellar temperature, indicating that the choice of damping should not adversely affect the differential analysis. We note that Prochaska et al. (2000) also see inconsistencies between these damping enhancements.

The choice of models with no convective overshoot was made both by taking into consideration the recommendations of Castelli et al. (1997) and by empirical testing. We first used models with convective overshoot, but we found a significant linear trend of increasing [Fe/H] with increasing $T_{\rm eff}$. Initially, we thought we were seeing the effects of uniform enrichment up the main sequence. However, the majority of our program stars are G and K dwarfs. Thus, if enrichment were uniform, there ought to be a plateau in the K and late G dwarfs with slight increase in early G and late F dwarfs. But this is not what we were seeing. The other concern was that the slope was large (roughly 0.15 dex from F to K), so we experimented with models with no convective

[5] Interpolation software was kindly supplied by A. McWilliam (1995, private communication) and updated by I. Ivans (2002, private communication).

TABLE 2
STELLAR PARAMETERS

HD	Other Name	$B-V$[a]	$T_{\rm eff}$ (K)	$\log g$ (cm s^{-2})	ξ (km s^{-1})	ζ[b] (km s^{-1})	$v \sin i$ (km s^{-1})
26784	vB 19	0.51	6450	4.2	1.1	4.89	15.7
27808	vB 48	0.52	6400	4.3	1.0	4.86	11.0
30809	vB 143	0.53	6400	4.2	0.9	4.79	10.1
28205	vB 65	0.54	6250	4.3	1.0	4.71	8.8
28635	vB 88	0.54	6250	4.3	0.8	4.69	1.0
26257	HIP 19386	0.55	6300	4.3	1.0	4.59	5.9
35768	HIP 25639	0.56	6300	4.3	1.0	4.57	4.4
27406	vB 31	0.56	6200	4.3	1.0	4.54	10.0
28237	vB 66	0.56	6250	4.3	0.7	4.54	8.6
20430	vB 1	0.57	6250	4.4	0.8	4.49	5.5
29419	vB 105	0.58	6100	4.4	0.8	4.42	2.5
30589	vB 118	0.58	6100	4.4	0.8	4.40	5.3
27835	vB 49	0.59	6050	4.4	0.8	4.31	2.8
25825	vB 10	0.59	6100	4.5	0.7	4.29	6.2
27859	vB 52	0.60	6050	4.4	0.5	4.24	6.5
28344	vB 73	0.61	6000	4.4	0.6	4.17	6.8
20439	vB 2	0.62	6050	4.4	0.6	4.11	5.5
28992	vB 97	0.63	5900	4.4	0.8	4.00	5.4
26767	vB 18	0.64	5900	4.4	0.8	3.94	5.4
26736	vB 15	0.66	5750	4.4	0.7	3.80	5.4
28099	vB 64	0.66	5800	4.4	0.7	3.75	3.4
26756	vB 17	0.69	5650	4.5	0.8	3.53	4.5
	HIP 13600	0.70	5600	4.5	0.6	3.44	1.8
27282	vB 27	0.72	5600	4.5	0.7	3.32	4.9
240648	HIP 23750	0.73	5600	4.5	0.7	3.25	4.9
19902	HIP 14976	0.73	5600	4.5	0.8	3.23	1.5
28593	vB 87	0.73	5550	4.5	0.8	3.22	4.0
31609	vB 127	0.74	5550	4.5	0.6	3.19	2.5
26015B.....	vB 12	0.74	5250	4.5	0.8	3.17	4.5
28805	vB 92	0.74	5500	4.5	0.7	3.17	3.8
27250	vB 26	0.75	5550	4.5	0.8	3.13	3.5
27732	vB 42	0.76	5500	4.5	0.8	3.03	3.8
32347	vB 187	0.77	5500	4.5	0.8	2.98	4.4
242780	HIP 24923	0.77	5500	4.5	0.7	2.98	4.8
283704	vB 76	0.77	5500	4.5	0.8	2.97	2.5
284574	vB 109	0.81	5350	4.5	0.8	2.63	4.6
284253	vB 21	0.81	5350	4.5	0.5	2.62	2.3
285773	vB 79	0.83	5300	4.5	0.5	2.48	3.4
30505	vB 116	0.83	5300	4.6	0.8	2.46	3.8
28258	vB 178	0.84	5350	4.6	0.7	2.42	3.5
	vB 4	0.84	5250	4.6	0.6	2.38	2.8
	vB 153	0.86	5200	4.6	0.7	2.30	3.8
27771	vB 46	0.86	5200	4.6	0.8	2.30	3.0
28462	vB 180	0.87	5250	4.6	1.0	2.22	3.9
29159	vB 99	0.87	5000	4.6	0.5	2.18	3.4
28878	vB 93	0.89	5150	4.6	0.7	2.03	3.8
285367	HIP 19098	0.89	5150	4.6	0.8	2.03	3.7
285252	vB 7	0.90	5050	4.6	0.8	1.99	3.8
	vB 5	0.92	5050	4.6	0.7	1.83	1.9
28977	vB 183	0.92	5150	4.6	0.9	1.80	3.5
18632	HIP 13976	0.93	5000	4.6	0.7	1.76	2.9
285830	vB 179	0.93	5050	4.6	0.6	1.73	3.6
	HIP 23312	0.96	5100	4.6	0.7	1.52	2.4
285690	vB 25	0.98	4900	4.6	0.8	1.35	2.5
14127	HIP 10672	0.57	6200	4.4	0.8	4.49	6.3

[a] $B-V$ values taken from Allende Prieto & Lambert 1999.
[b] Macroturbulence derived from Saar & Osten 1997.

overshoot. The trend of abundance with $T_{\rm eff}$ disappeared by using these models. Thus, we decided to use models with no overshoot for the entire analysis.

For each star, we measured the EWs of 12–20 (presumably) unblended Fe I lines and 5–9 unblended Fe II lines in the region 4490–6175 Å. We preferentially chose lines redward of 4500 Å because of the extremely crowded spectra blueward of this cutoff. Where possible we tried to maintain only lines that were significantly redward of this. Continuum placement becomes difficult in the blue end of the

TABLE 3
Elemental Abundances

HD	Other Name	[Fe/H]	[Na/Fe]	[Mg/Fe]	[Si/Fe]	[Ca/Fe]	[Ti/Fe]	[Zn/Fe]
26784	vB 19	0.23	0.07	−0.08	−0.01	0.08	0.08	−0.19
27808	vB 48	0.15	0.07	0.00	0.06	0.15	0.15	0.11
30809	vB 143	0.19	0.10	−0.06	0.02	0.29	0.15	−0.14
28205	vB 65	0.10	0.03	−0.08	0.08	0.17	0.10	−0.05
28635	vB 88	0.09	0.05	−0.05	0.05	0.11	0.01	−0.09
26257	HIP 19386	0.11	0.00	−0.11	0.09	0.12	0.03	−0.03
35768	HIP 25639	0.08	0.08	−0.02	0.05	0.12	0.12	−0.10
27406	vB 31	0.15	0.05	−0.06	0.01	0.19	0.07	−0.06
28237	vB 66	0.14	0.04	−0.01	0.02	0.22	0.03	0.04
20430	vB 1	0.30	0.02	−0.05	0.00	0.16	0.07	−0.11
29419	vB 105	0.13	−0.06	−0.05	0.01	0.11	−0.04	−0.07
30589	vB 118	0.15	0.00	−0.08	0.02	0.09	0.00	−0.12
27835	vB 49	0.09	0.00	−0.06	0.05	0.10	0.03	−0.08
25825	vB 10	0.15	0.02	−0.07	−0.04	0.12	−0.03	−0.01
27859	vB 52	0.14	0.01	−0.05	0.00	0.13	0.03	0.02
28344	vB 73	0.18	0.01	−0.09	−0.03	0.11	0.01	0.00
20439	vB 2	0.30	0.01	−0.06	−0.02	0.13	0.04	−0.03
28992	vB 97	0.12	−0.01	−0.11	0.02	0.09	0.03	−0.05
26767	vB 18	0.12	−0.01	−0.01	0.04	0.13	0.05	0.00
26736	vB 15	0.09	0.05	0.01	0.06	0.14	0.00	0.08
28099	vB 64	0.10	0.02	−0.04	0.05	0.11	0.04	−0.04
26756	vB 17	0.06	0.01	−0.03	0.08	0.08	0.02	−0.08
	HIP 13600	0.02	0.03	0.02	0.04	0.09	0.03	−0.04
27282	vB 27	0.15	0.01	−0.01	0.03	0.08	0.05	−0.03
240648	HIP 23750	0.15	−0.01	−0.05	0.02	0.09	0.03	−0.02
19902	HIP 14976	0.09	0.00	−0.06	0.07	0.05	0.03	−0.08
28593	vB 87	0.11	0.02	−0.07	0.06	0.03	0.02	−0.08
31609	vB 127	0.15	0.01	−0.08	0.00	0.02	−0.01	−0.10
26015B.....	vB 12	0.17	−0.04	−0.07	0.00	−0.01	−0.01	−0.09
28805	vB 92	0.08	−0.04	−0.05	0.06	0.06	−0.04	−0.02
27250	vB 26	0.09	−0.02	0.00	0.09	0.04	0.06	−0.09
27732	vB 42	0.10	−0.05	−0.04	0.06	0.08	−0.04	−0.06
32347	vB 187	0.11	−0.05	−0.02	0.06	0.09	0.03	−0.05
242780	HIP 24923	0.12	0.02	−0.05	0.07	0.09	0.07	−0.04
283704	vB 76	0.09	0.01	−0.04	0.07	0.06	0.03	−0.07
284574	vB 109	0.13	0.01	−0.04	0.08	0.08	0.05	0.00
284253	vB 21	0.14	0.02	−0.06	0.00	0.06	0.02	−0.05
285773	vB 79	0.14	0.01	−0.09	0.02	0.02	0.00	−0.06
30505	vB 116	0.13	−0.05	−0.09	0.05	0.02	0.03	−0.07
28258	vB 178	0.15	−0.03	−0.06	0.02	0.05	−0.02	−0.09
	vB 4	0.15	−0.02	−0.09	0.02	0.02	0.03	−0.07
	vB 153	0.10	−0.03	−0.04	0.07	0.06	0.07	−0.01
27771	vB 46	0.08	0.00	−0.07	0.14	0.00	0.05	−0.01
28462	vB 180	0.08	−0.02	−0.02	0.09	0.01	0.03	−0.08
29159	vB 99	0.09	0.04	−0.13	0.17	−0.12	0.05	0.03
28878	vB 93	0.13	−0.05	−0.09	0.06	0.01	0.01	−0.05
285367	HIP 19098	0.11	−0.05	−0.08	0.05	0.03	0.02	−0.10
285252	vB 7	0.15	−0.03	−0.11	0.10	−0.08	−0.06	−0.07
	vB 5	0.16	−0.08	−0.12	0.04	−0.05	−0.01	−0.13
28977	vB 183	0.13	−0.01	−0.09	0.03	0.03	0.07	−0.14
18632	HIP 13976	0.18	−0.10	−0.10	0.06	−0.02	0.03	−0.15
285830	vB 179	0.22	−0.08	−0.15	0.03	−0.03	0.03	−0.12
	HIP 23312	0.18	−0.04	−0.11	−0.04	0.00	0.09	−0.20
285690	vB 25	0.08	−0.08	−0.06	0.20	−0.03	0.02	−0.09
14127	HIP 10672	−0.12	−0.09	−0.01	0.02	0.14	0.10	−0.05

spectrum. The number of lines available varied according to the temperature of the star. Because the emphasis of this work is differential, absolute accuracy of elemental *gf* values are of less importance. However, in order to obtain correct stellar parameters, we wanted to use accurate Fe *gf* values. In the same way all EWs were measured, we varied the *gf* values until the line abundances matched the solar model and solar abundances. We used the Kurucz solar atlas (Kurucz, Furenlid, & Brault 1984) for this analysis.

In 2001 December, C. Allende Prieto obtained spectra of several super–solar mass Hyades stars with McDonald Observatory's 2.7 m Harlan Smith telescope using the coudé echelle spectrograph ($R = 60,000$ with S/N of about 300–500 per pixel at 5800 Å). Of these stars, 11 were also

TABLE 4
COMPARISON OF DERIVED PARAMETERS FOR STARS COMMON TO BOTH SAMPLES

Star	Δ[Fe/H]	$\Delta T_{\rm eff}$ (K)	$\Delta \log g$	$\Delta\xi$ (km s^{-1})
vB 19.....	0.06	0	0	0.1
vB 10.....	0.03	0	0	0
vB 73.....	0.04	0	0	0
vB 118.....	0.06	50	0	0
vB 105.....	0.08	0	−0.1	−0.1
vB 66.....	0.03	0	0	0
vB 88.....	0.07	50	0	−0.1
vB 65.....	0.09	0	0	−0.1
vB 143.....	0.06	0	−0.1	−0.1
vB 48.....	0.01	0	0	0
vB 31.....	0.07	0	0	−0.1

observed in our sample at Keck, providing a comparison and check of measurements of stellar parameters between the data sets. The stars observed at McDonald are typically higher mass, and thus higher $v \sin i$, than the stars chosen for planet search at Keck. So, several of the stars observed by C. Allende Prieto are not easily analyzed with the equivalent width method for determining abundances using the chosen line list. We do not want to compromise the internal consistency of this analysis by adopting a separate line list for this additional set of data. Therefore, in this paper, we only discuss the analysis of the 11 stars common to both data sets.

We compare the stellar parameters derived for these 11 stars in Table 4. EWs measured from the McDonald spectra tend to be, on average, a few mÅ larger than the Keck spectra. This yields slightly higher (roughly 0.05 dex) abundances for [Fe/H]. This enhancement is completely due to the use of different spectrographs. In general, the stellar parameters we derive are consistent between the two data sets.

Our determination of $T_{\rm eff}$ also agrees well with the $T_{\rm eff}$ derived for stars in common with Allende Prieto & Lambert (1999) as shown in Figure 2, noting that Allende Prieto & Lambert list log $T_{\rm eff}$ rounded to 2 decimal places. Thus, in Figure 2 the converted $T_{\rm eff}$ from Allende Prieto & Lambert values appear to be in discrete units. The mean difference is $\langle T_{\rm eff,\,this\ study} - T_{\rm eff,\,Allende\text{-}Prieto} \rangle = 34.6$ K, with a standard deviation $\sigma = 67.9$ K.

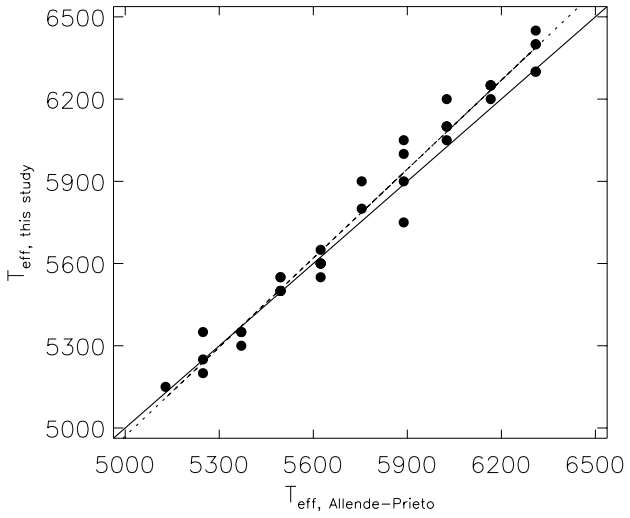

FIG. 2.—Comparison of $T_{\rm eff}$ derived in this study vs. those derived by Allende Prieto & Lambert (1999). The solid line is 1 : 1, and the dashed line is a least-squares fit to the data.

3.2. [Fe/H] *and* [X/Fe]

Absolute [Fe/H] abundances are derived during the process of determining stellar parameters. Using the derived stellar atmosphere models and measured EWs of various atomic lines listed in Table 1, we determined elemental abundances ([X/Fe]). Derived [Fe/H] and [X/Fe] values are listed for each star in Table 3.

Our derived mean Hyades metallicity is $\langle [{\rm Fe/H}] \rangle = 0.13 \pm 0.01$ with $\sigma = 0.05$, not including HD 14127. If we also exclude vB 1 and vB 2, we obtain $\langle [{\rm Fe/H}] \rangle = 0.13 \pm 0.01$, $\sigma = 0.04$. This is in agreement with various surveys of Hyades metallicity, e.g., $\langle [{\rm Fe/H}] \rangle = 0.16 \pm 0.04$ (Boesgaard, Beard, & King 2002), 0.20 ± 0.10 (Branch et al. 1980), 0.130 ± 0.026 (Boss 1989), and 0.12 ± 0.03 (Cayrel et al. 1985).

We now consider the stars with [Fe/H] not within 1 σ of the cluster mean (these outliers can be seen in the differential [Fe/H] plot of Figure 3, which is further discussed in § 3.3). The two outliers with Δ[Fe/H] (and [Fe/H]) lower than the cluster mean (*dashed line*), HD 14127 and HIP 13600, are disregarded because of questionable membership, as discussed in § 3.6.

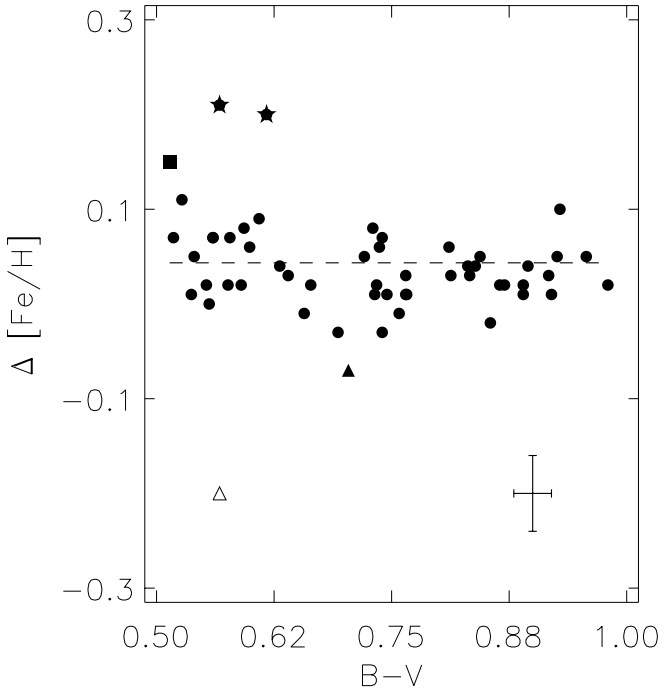

FIG. 3.—Differential [Fe/H] of sample stars vs. $B-V$. The differential comparison star is vB 153, as discussed in the text. Note that the on every low outlier is HD 14127 (*open triangle*), and HIP 13600 (*filled triangle*) is just slightly lower in [Fe/H] than the other members. It can be seen that vB 1, vB 2 (*filled stars*), and vB 19 (*filled square*) all are higher than other members. See § 3.6 for membership information. The dashed line is the mean abundance level. A set of typical error bars for each measurement is shown in the bottom right corner of the plot.

One might assume that for the outliers with high [Fe/H] (and Δ[Fe/H]) (vB 19, vB 1, and vB 2, as seen in Fig. 3) that we have determined an incorrect set of model parameters—that, perhaps, our determined $T_{\rm eff}$ are too high. However, changing the model parameters by reasonable amounts cannot solve the entire problem of their high abundances. For vB 19, the determination of log g may be questionable because of the fact that we were only able to measure four Fe II lines in the spectrum. If the gravity is questionable, then the other parameters may be off slightly as well. We have derived a $T_{\rm eff}$ that is roughly 150 K higher than Allende Prieto & Lambert (1999, hereafter APL99) derived. We note that APL99 interpolate theoretical isochrones with observed data from *Hipparcos* to get stellar parameters, which is a different approach from the one we use. Thus, some amount of disagreement is understandable between our study and theirs. To test our abundance determination, however, we force vB 19 to have APL99's derived temperature and rederive the other stellar parameters. We find $\xi = 1.0$ km s^{-1} and $\log g = 3.9$. Together, these new parameters give an [Fe/H] of 0.16. This is within 1 σ of the cluster mean, although still on the high end. However, the new gravity derived is in strong disagreement with 4.40 as derived by APL99. So, assuming that the disagreement in log g can be explained by EW measurement error, the high abundance in vB 19 may be reduced to within 1 σ of the cluster mean. Thus, we do not feel strongly that vB 19 is, indeed, enhanced relative to the cluster.

Doing the same test for vB 1, forcing a $T_{\rm eff}$ of 6165 K gives log g of 4.1 (in disagreement with APL99's 4.51), ξ of 0.8 km s^{-1}, and [Fe/H] of 0.23, still significantly higher than the cluster mean. For the final case of vB 2, forcing the $T_{\rm eff}$ to be 5888 K gives log g of 4.1 (APL99 derived 4.40), ξ of 0.6 km s^{-1}, and [Fe/H] of 0.24 (also significantly higher than the cluster mean). So, the high abundances of vB 1 and vB 2 cannot simply be explained by poor choice of models unless the true model parameters are drastically inconsistent with what we have measured. In addition, in his initial analysis Fulbright (2002) also sees an enrichment in these two stars. So, either vB 1 and vB 2 are not members or they have been enriched relative to the cluster mean. The membership of these stars is further discussed in § 3.6.

3.3. *Differential* [Fe/H] *and* [X/Fe]

By employing a differential abundance analysis (e.g., Gray 1992), one removes the uncertainty in the oscillator strengths of the lines, which are often poorly known. Therefore, to answer the question of whether we see enrichment of metals within the Hyades cluster, we use a self-consistent, differential abundance analysis to look for any star-to-star metallicity variations. We do not employ the method of also deriving differential stellar parameters as Laws & Gonzalez (2001) do, because our $T_{\rm eff}$ range is too large. By doing a line-by-line differential analysis, we will be able to place upper limits on the amount of H deficient debris that could have been accreted onto a star's photosphere relative to the cluster mean.

In order to get differential abundances (Δ[Fe/H] and Δ[X/Fe]), we subtract log ϵ(X) of each line in each star with the same line in a comparison star (we chose the K dwarf vB 153). Thus, Δ[Fe/H] and Δ[X/Fe] are the means of the differences for all lines in a given star. The scatter is significantly reduced. This gives a more accurate relative abundance than we can obtain by just taking the mean of all lines and subtracting that value from solar (the values [Fe/H] and [X/Fe]). Differential abundance values are listed in Table 5 and are plotted in Figures 3 and 4 for each species,

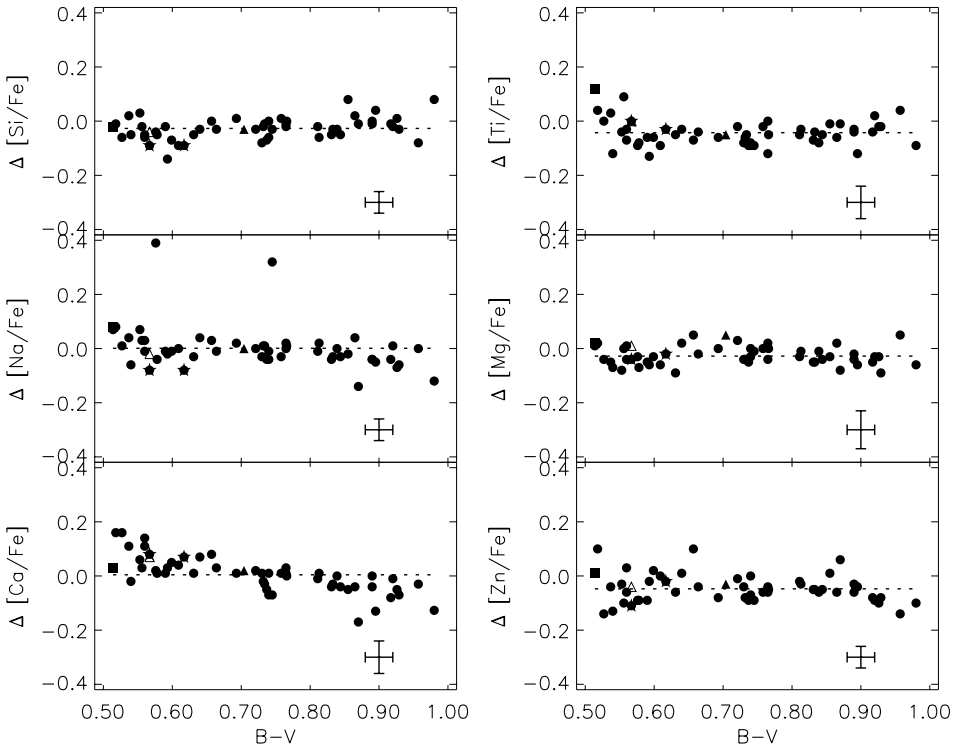

FIG. 4.—Differential [X/Fe] of sample stars vs. $B-V$. The differential comparison star is vB 153, as discussed in the text. The symbols are the same as in Fig. 3. Dashed lines are mean abundance levels. Typical error bars are shown in each panel in the bottom right corner.

TABLE 5
Differential Abundances

HD	Other Name	Δ[Fe/H]	Δ[Na/Fe]	Δ[Mg/Fe]	Δ[Si/Fe]	Δ[Ca/Fe]	Δ[Ti/Fe]	Δ[Zn/Fe]
26784	vB 19	0.15	0.08	0.02	−0.02	0.03	0.12	0.01
27808	vB 48	0.07	0.08	0.02	−0.01	0.16	0.04	0.10
30809	vB 143	0.11	0.01	−0.04	−0.06	0.16	0.00	−0.14
28205	vB 65	0.01	0.04	−0.05	0.02	0.11	0.03	−0.04
28635	vB 88	0.05	−0.06	−0.07	−0.05	−0.02	−0.12	−0.13
26257	HIP 19386	0.02	0.07	−0.08	0.03	0.06	−0.04	−0.03
35768	HIP 25639	0.00	0.03	0.00	−0.02	0.03	0.09	−0.10
27406	vB 31	0.07	0.03	−0.04	−0.05	0.11	−0.03	−0.06
28237	vB 66	0.07	−0.01	0.01	−0.06	0.14	−0.07	0.03
20430	vB 1	0.21	−0.08	−0.04	−0.09	0.08	0.00	−0.11
29419	vB 105	0.04	0.39	−0.03	−0.04	0.02	−0.09	−0.09
30589	vB 118	0.07	−0.03	−0.07	−0.05	0.01	−0.08	0.09
27835	vB 49	0.02	−0.01	−0.05	−0.02	0.01	−0.06	−0.09
25825	vB 10	0.08	−0.02	−0.06	−0.14	0.03	−0.13	−0.02
27859	vB 52	0.06	−0.01	−0.03	−0.07	0.05	−0.06	0.02
28344	vB 73	0.09	0.00	−0.06	−0.09	0.04	−0.09	0.00
20439	vB 2	0.20	−0.08	−0.02	−0.09	0.07	−0.03	−0.02
28992	vB 97	0.04	−0.03	−0.09	−0.05	0.01	−0.05	−0.06
26767	vB 18	0.03	0.04	0.02	−0.03	0.07	−0.03	0.01
26736	vB 15	−0.01	0.03	0.05	0.00	0.08	−0.07	0.00
28099	vB 64	0.02	−0.01	−0.02	−0.03	0.03	−0.04	0.10
26756	vB 17	−0.03	0.02	0.00	0.01	0.01	−0.06	−0.08
	HIP 13600	−0.07	0.00	0.05	−0.03	0.02	−0.05	−0.03
27282	vB 27	0.05	0.00	0.03	−0.03	0.02	−0.02	−0.01
240648	HIP 23750	0.08	−0.03	−0.04	−0.08	0.01	−0.08	−0.04
19902	HIP 14976	0.01	0.01	−0.04	−0.02	−0.02	−0.06	−0.08
28593	vB 87	0.02	0.01	−0.04	−0.01	−0.03	−0.05	−0.08
31609	vB 127	0.06	−0.04	−0.05	−0.07	−0.05	−0.09	−0.09
26015B.....	vB 12	0.07	−0.04	−0.03	−0.06	−0.07	−0.08	−0.07
28805	vB 92	−0.03	−0.01	0.00	0.00	0.01	−0.09	0.00
27250	vB 26	0.01	0.32	−0.01	−0.03	−0.07	−0.09	−0.09
27732	vB 42	−0.03	−0.01	0.00	0.01	0.01	−0.02	−0.06
32347	vB 187	0.01	0.02	0.02	−0.02	0.03	−0.12	−0.04
242780	HIP 24923	0.03	0.00	−0.04	−0.01	0.01	0.00	−0.06
283704	vB 76	−0.01	0.01	0.00	0.00	0.00	−0.05	−0.05
284574	vB 109	0.06	−0.01	−0.03	−0.02	−0.01	−0.05	−0.02
284253	vB 21	0.03	0.02	−0.01	−0.06	0.01	−0.03	−0.03
285773	vB 79	0.04	−0.04	−0.05	−0.05	−0.04	−0.07	−0.05
30505	vB 116	0.03	−0.03	−0.05	−0.03	−0.03	−0.04	−0.05
28258	vB 178	0.04	0.00	−0.01	−0.03	0.00	−0.08	−0.06
	vB 4	0.05	−0.03	0.04	−0.05	0.04	−0.05	−0.05
	vB 153	...	...	...	...	...	...	...
27771	vB 46	−0.02	−0.02	−0.03	0.08	−0.05	−0.01	0.01
28462	vB 180	−0.02	0.04	0.02	0.02	−0.04	−0.06	−0.06
29159	vB 99	−0.02	−0.14	−0.08	−0.01	−0.17	−0.01	0.06
28878	vB 93	0.02	−0.04	−0.04	−0.01	−0.04	−0.04	−0.03
285367	HIP 19098	−0.01	−0.04	−0.02	0.00	0.00	−0.03	−0.06
285252	vB 7	0.04	−0.05	−0.06	0.04	−0.13	−0.12	−0.04
	vB 5	0.03	−0.04	−0.05	−0.01	−0.08	−0.04	−0.08
28977	vB 183	0.01	0.01	−0.03	−0.02	−0.01	0.02	−0.09
18632	HIP 13976	0.05	−0.07	−0.03	0.01	−0.05	−0.02	−0.10
285830	vB 179	0.10	−0.06	−0.09	−0.03	−0.07	−0.02	−0.08
	HIP 23312	0.05	0.00	0.05	−0.08	−0.03	0.04	−0.14
285690	vB 25	0.02	−0.12	−0.06	0.08	−0.12	−0.09	−0.10
14127	HIP 10672	−0.20	−0.02	0.01	−0.04	0.07	0.00	−0.04

with typical error bars shown in the bottom right corner of each panel. For a given element, we determine the star-to-star variations with a standard deviation about the mean $\sigma \leq 0.05$ dex and the standard deviation of the mean significantly lower (<0.01 dex). The Δ[Si/Fe], Δ[Ti/Fe], Δ[Na/Fe], Δ[Mg/Fe], and Δ[Zn/Fe] are all fairly consistent with Δ[Fe/H]; they are constant along the main sequence with small scatter. The linear least-squares fits to these data reveal the following relationships:

$$\Delta[\mathrm{Si/Fe}] = -0.106 + 0.109(B-V)\ ,$$
$$\Delta[\mathrm{Ti/Fe}] = -0.014 - 0.040(B-V)\ ,$$
$$\Delta[\mathrm{Na/Fe}] = 0.087 - 0.129(B-V)\ ,$$
$$\Delta[\mathrm{Mg/Fe}] = -0.025 - 0.004(B-V)\ ,$$
$$\Delta[\mathrm{Zn/Fe}] = 0.001 - 0.067(B-V)\ .$$

TABLE 6
Mean Cluster Abundances

Measurement	⟨[Fe/H]⟩	⟨[Na/Fe]⟩	⟨[Mg/Fe]⟩	⟨[Si/Fe]⟩	⟨[Ca/Fe]⟩	⟨[Ti/Fe]⟩	⟨[Zn/Fe]⟩
Absolute	0.13	0.01	−0.06	0.05	0.07	0.03	−0.06
σ.....	0.05	0.09	0.04	0.05	0.07	0.05	0.06
Differential.....	0.04	−0.01	−0.03	−0.03	0.01	−0.04	−0.05
σ.....	0.05	0.06	0.04	0.04	0.07	0.05	0.05

In addition, Δ[Ca/Fe] has a significant trend in abundance with color. The value of Δ[Ca/Fe] is zero at the same $B-V$ as the comparison star. Therefore, we believe this trend is primarily due to the fact that these lines begin to move off the linear part of the curve of growth (start becoming saturated) in cooler stars. For the other elements, when a line had this type of behavior, we removed it from the list (we preferred to maintain one line list for the entire sample of stars). However, there was not a reasonable number of lines available for us to remove all lines of Ca that behave like this. The least-squares fit for Ca is $\Delta[\mathrm{Ca/Fe}] = 0.274 - 0.372(B-V)$.

In Figure 4, there are two severe outliers. In the Δ[Na/Fe] plot, vB 26 and vB 105 have extremely high Δ[Na/Fe] compared to the cluster. The cause of this enhancement is saved for future study.

Finally, Table 6 lists cluster mean abundances for both absolute and differential analyses.

3.4. *v sin i*

We also determine the rotational velocity ($v \sin i$) for all stars. The $v \sin i$, the instrumental profile (IP), the macroturbulence (ζ), and the limb darkening are combined to form a "smoothing" parameter. This smoothing parameter is convolved with an intensity profile for the star. Because we derive an intensity profile from the stellar models, in order to determine $v \sin i$, we only need to determine these other broadening parameters. We synthesized five Fe I lines in this 6150–6180 Å region. For each line, we know the abundance from determination of the stellar parameters. We then fit a "smoothing" parameter to each line including calculated, measured, or estimated values for each of the other broadening parameters. The IP is measured by fitting a Gaussian to the lines of the thorium-argon (ThAr) calibration lamp. The FWHM, as measured from the ThAr calibration spectra, varies from 0.0918 to 0.0921 Å from the redmost to the bluemost lines in the chosen region. The synthesis code is insensitive to this small a change. We thus used 0.09 Å as the IP broadening. We estimated ζ according to the Saar & Osten (1997) estimates for active stars and using $B-V$ from APL99. The limb-darkening coefficient is estimated from Gray (1992). Using the individual abundances and the above smoothing parameters, the only unknown left is $v \sin i$. We took a mean of the $v \sin i$ derived for each of the five lines to determine the overall $v \sin i$ of the star. In this manner, we are able to determine $v \sin i$ to about 0.7 km s^{-1}.

The upper panel of Figure 5 shows $v \sin i$ versus $B-V$ for our target stars, and individual measurements of $v \sin i$ are listed in Table 2. We see the expected decrease of $v \sin i$ with decreasing mass and the expected spread due to the $\sin i$ ambiguity. To estimate the actual rotational velocity of a star in the cluster based solely on color (or mass or $T_{\rm eff}$) we only need to fit a function to the upper envelope of the $v \sin i$ data. In Figure 5 we have done so for three different functions *for our data alone*. The best fit for our data was with a fifth-order polynomial (Fig. 5, *solid curve*). The second panel in Figure 5 shows our $v \sin i$ measurements and fits to our data along with $v \sin i$ from Böhm-Vitense et al. (2002), Benz , Mayor, & Mermilliod (1984) (with $B-V$ values from SIMBAD[6]), and selected dwarfs from Kraft (1965). The $v \sin i$ values taken from literature were measured in different ways, and typically they do not remove the, albeit small, contribution of macroturbulence. Our fits (Fig. 5, *solid, dashed, and dotted lines*) do not take into account the $v \sin i$ values from literature. These fits are extended to show that, while consistent with our data, they do not correctly quantify the true rotational velocity "upper envelope" for all Hyades stars.

[6] This research has made use of the SIMBAD database, operated at CDS, Strasbourg, France.

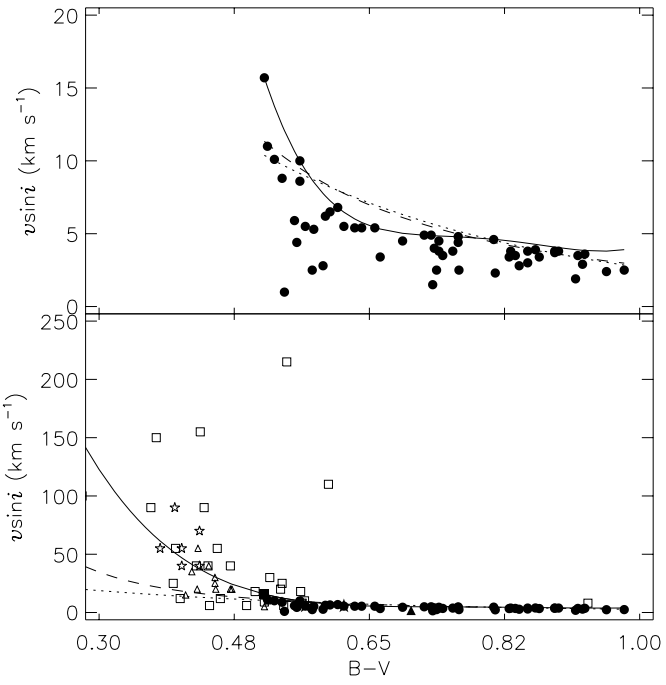

Fig. 5.—Plot of $v \sin i$ of observed Hyades stars (including the same possible nonmembers, as discussed in Fig. 3). The symbols are the same as in Figure 3. The solid curve is a polynomial fit to the upper envelope of our data (*filled circles*) as discussed in the text; the dashed curve is a power law to our data only, and the dotted curve is an exponential fit to our data, as well. The upper panel shows only our data, while the bottom panel adds in $v \sin i$ measurements from Böhm-Vitense et al. (2002) (*open triangles*), Benz et al. (1984) (*open stars*), and selected dwarfs from Kraft (1965) (*open squares*).

3.5. *Errors*

There are several sources of error when measuring stellar abundances, especially if one is interested in absolute abundances. External errors such as uncertainties in atomic parameters, choice of model atmospheres, and solar abundances can cause significant errors in determined absolute abundances, while these are minimized in differential abundance analysis. Internal errors such as measurement of stellar absorption lines, continuum placement, and choice of stellar model parameters can be minimized and quantified to some degree. Typically, we can reliably measure EWs to $\lesssim 1$ mÅ. On average, an overestimation of a single line's EW by 1 mÅ will give a higher line abundance by 0.02 dex. Individual cases obviously will depend on the S/N of the spectra (i.e., spectra with higher levels of noise will have larger errors in EW determination). Lines having noise that caused problems in line fitting (i.e., where a noise spike was present in the line or where the feature was difficult to discern from the noise in the continuum) were not included in the analysis. Continuum placement is also a (somewhat) unquantifiable source of error. However, as an example, we changed the order of the cubic spline fit to the continuum for a given spectrum and measured the EW from the same set of lines. A change from a third-order to a fifth-order spline gave a decrease in the EW of, on average, 0.4 mÅ. In addition, we can quantify some internal errors, even though most of the fitting for the parameters ($T_{\rm eff}$, ξ, and $\log g$) are done by eye. Table 7 shows the abundance dependencies on model parameters. For Mg abundance determination we were only able to measure one stellar line, for Zn and Na two lines, and for Ca only three. The absolute abundances quoted here for these elements are much less certain than, say, Fe, which has significantly many more lines. For absolute [Fe/H], [Ti/H], and [Si/H], the *total* error on an individual measurement is about 0.1 dex, which includes both internal and external errors. Differentially, the uncertainties are much smaller, on the order of 0.05 dex. This is smaller because of the removal of certain external errors such as the atomic *gf* parameter.

3.6. *Notes on Cluster Membership*

The following nine stars have at least one anomalous characteristic compared to other cluster members. The stellar characteristics of interest here are metallicity, chromospheric activity level, photometry, proper motion, and parallax.

HD 14127 was included as a member by Perryman et al. (1998, hereafter Pe98) based on *Hipparcos* observations. D. Latham (1999, private communication) concluded that this star is not a member because it has too high a *Hipparcos* distance and the photometry is below the main sequence. In Paulson et al. (2002, hereafter Pa02), we showed that this star does have activity levels consistent with the age of the Hyades. However, this star's metallicity is 0.25 dex below the cluster mean. Thus, it is severely inconsistent with the Hyades. It is our belief that this star is not a member of the Hyades.

HIP 13600 has slightly low abundances in all elements but Mg. In the activity analysis, it was also an outlier, showing much lower activity levels than expected for a Hyades member (Pa02). Again, this star was included by Pe98, but Latham concludes that the photometry is below the main sequence and the *Hipparcos* distance is too high. Hoogerwerf & Aguilar (1999) reject this star as a cluster member. Thus, we consider HIP 13600 is a probable nonmember.

vB 118, HD 26257, HD 35768, and HD 19902 all show low activity levels (Pa02), but in this analysis they all have metallicities consistent with the Hyades cluster mean. Of these, Latham concludes that HD 26257, HD 35768, and HD 19902 are not members based on the same criterion as above. He agrees that vB 118 is a member. Pe98 includes all of these stars as members. HD 26257 and HD 35768 were rejected by Hoogerwerf & Aguilar, and HD 35768 was also rejected by de Bruijne, Hoogerwerf, & de Zeeuw (2001). At this point, we still consider vB 118 to be a member. The others are considered to be probable nonmembers.

vB 12, also showing consistent abundances and photometry, radial velocity and *Hipparcos* distances, shows slightly high activity levels. We believe that this star is most likely a cluster member despite its anomalous activity level.

vB 1 and vB 2 are the two stars in the sample that have significantly higher abundances than the cluster mean. They both have consistent photometry, radial velocity, and *Hipparcos* distances for membership. vB 1 has a slightly low activity level as compared to the cluster mean. De Bruijne et al. (2001) find that these stars are nonmembers based on the proper motion and trigonometric parallax analyses of both de Bruijne (1999) and Hoogerwerf & Aguilar (1999). The radial velocities of both of these stars is 31 km s^{-1}, well within the range of the cluster (28–42 km s^{-1}). They have similar proper motions and are near one another in the cluster (the difference in right ascension is $6^{\rm s}.39$ and only $2^{\rm m}3^{\rm s}.6$ in declination). Our differential radial velocity curves of these two stars (which, admittedly, only spans $\sim$5 yr) do not reveal any linear trends suggesting a relationship between them, although the possibility still remains that they are or once were a wide binary pair. It is also well known that nearby solar-type stars are generally of solar metallicity or lower; for example, see the recent survey by Gaidos & Gonzalez (2002). So it is unlikely that these stars happen to have similar supersolar metallicities, are quite close in proximity,

TABLE 7
ABUNDANCE DEPENDENCIES ON MODEL PARAMETERS

Example Star	Model Parameter	δ[Fe/H]	δ[Na/Fe]	δ[Mg/Fe]	δ[Si/Fe]	δ[Ca/Fe]	δ[Ti/Fe]	δ[Zn/Fe]
vB 65 ($T_{\rm eff} = 6250$).....	$T_{\rm eff} \pm 50$	$\pm$0.04	$\mp$0.02	$\pm$0.01	$\mp$0.02	$\mp$0.01	$\pm$0.01	$\mp$0.01
	$\log g \pm 0.20$	$\pm$0.04	$\mp$0.01	$\mp$0.02	$\mp$0.01	$\mp$0.02	$\mp$0.01	0.00
	$\xi \pm 0.2$	$\mp$0.03	$\pm$0.02	0.00	$\pm$0.01	$\mp$0.01	$\mp$0.02	$\mp$0.06
vB 7 ($T_{\rm eff} = 5050$)	$T_{\rm eff} \pm 50$	$\pm$0.01	$\pm$0.03	$\pm$0.01	$\mp$0.03	$\pm$0.03	$\pm$0.05	$\mp$0.03
	$\log g \pm 0.2$	$\pm$0.01	$\mp$0.06	$\mp$0.07	$\pm$0.01	$\mp$0.09	$\mp$0.02	$\mp$0.01
	$\xi \pm 0.2$	$\mp$0.04	$\pm$0.02	$\mp$0.01	$\pm$0.02	0.00	$\mp$0.02	$\mp$0.01

and are just random field stars. We consider these stars to have questionable membership, but at this time we are not able to make a more solid classification.

4. DISCUSSION

It is apparent now that at the 1 σ (or 0.04 dex) level, most Hyades members are uniform in composition. The abundances of several elements were measured to support this assertion. The implication of this result is that because the Hyades members were formed from homogeneous material, if significant enrichment of photospheres occurred, we would be able to see evidence of the enrichment. And since we do not see variations in measured abundances, significant enrichment has not occurred in these stars. Recalling the calculations of Pinsonneault et al. (2001), enrichment of 10 $M_{\oplus}$ of Fe will increase the stellar [Fe/H] by 0.09 dex. We are able to rule out enrichment of this magnitude in our higher mass stars. We are able to scale this relation and determine that we still do not see enrichment at even the 7 $M_{\oplus}$ level.

vB 1 and vB 2 are interesting stars. They are significantly enriched relative to the cluster mean. Early surveys have always included them as members, but recently, de Bruijne et al. (2001) assert that they are nonmembers. The question remains, then, whether these stars are enriched members or whether they are interlopers. These two stars certainly merit significant further study.

When the search for planets concludes, we will be able to say more firmly whether planets exist in the Hyades and, if they have migrated, we will be able to place firm upper limits on the amount of debris that could have been cast onto the star during this process. For now, we are only able to place upper limits on the possible enrichment due to possible disks. Moreover, we are confident that the material that formed member stars was, in fact, homogeneous.

We would like to thank Carlos Allende Prieto and David Yong for use of data obtained at McDonald Observatory. In addition, D. B. P. would like to thank Jennifer Simmerer for many useful discussions about stellar abundance analysis. This material is based upon work supported by the National Aeronautics and Space Administration under grant NAG5-9227 issued through the Office of Space Science. C. S. is supported by NSF grant AST 99-87162.

REFERENCES

Allende Prieto, C., & Lambert, D. L. 1999, A&A, 352, 555 (APL99)
Benz, W., Mayor, M., & Mermilliod, J. C. 1984, A&A, 138, 93
Blackwell, D. E., Lynas-Gray, A. E., & Smith, G. 1995, A&A, 296, 217
Boesgaard, A. M., Beard, J. L., & King, J. R. 2002, BAAS, 34, 1170
Boesgaard, A. M., & Budge, K. G. 1988, ApJ, 332, 410
Boesgaard, A. M., Heacox, W. D., & Conti, P. S. 1977, ApJ, 214, 124
Böhm-Vitense, E., Robinson, R., Carpenter, K., & Mena-Werth, J. 2002, ApJ, 569, 941
Boss, A. P. 1989, PASP, 101, 767
Branch, D., Lambert, D. L., & Tomkin, J. 1980, ApJ, 241, L83
Burkhart, C., & Coupry, M. F. 1989, A&A, 220, 197
———. 2000, A&A, 354, 216
Castelli, F., Gratton, R. G., & Kurucz, R. L. 1997, A&A, 318, 841
Cayrel, R., Cayrel de Strobel, G., & Campbell, B. 1985, A&A, 146, 249
Chaffee, F. H., Carbon, D. F., & Strom, S. E. 1971, ApJ, 166, 593
Cochran, W. D., Hatzes, A. P., & Paulson, D. B. 2002, AJ, 124, 565
Conti, P. S., Wallerstein, G., & Wing, R. F. 1965, ApJ, 142, 999
de Bruijne, J. H. J. 1999, MNRAS, 306, 381
de Bruijne, J. H. J., Hoogerwerf, R., & de Zeeuw, P. T. 2001, A&A, 367, 111
Friel, E. D., & Boesgaard, A. M. 1990, ApJ, 351, 480
Fulbright, J. P. 2002, BAAS, 34, 1128
Gaidos, E. J., & Gonzalez, G. 2002, NewA, 7, 211
Garcia Lopez, R. J., Rebolo, R., Herrero, A., & Beckman, J. E. 1993, ApJ, 412, 173
Gonzalez, G. 1997, MNRAS, 285, 403
———. 1998, A&A, 334, 221
Gratton, R. G., Bonanno, G., Claudi, R. U., Cosentino, R., Desidera, S., Lucatello, S., & Scuderi, S. 2001, A&A, 377, 123
Gray, D. F. 1992, The Observation and Analysis of Stellar Photospheres (Cambridge: Cambridge Univ. Press)
Grevesse, N., & Sauval, A. J. 1998, Space Sci. Rev., 85, 161
Holweger, H. 1971, A&A, 10, 128
Hoogerwerf, R., & Aguilar, L. A. 1999, MNRAS, 306, 394
Hui-Bon-Hoa, A., & Alecian, G. 1998, A&A, 332, 224
Jeffery, C. S., Bailey, M. E., & Chambers, J. E. 1997, Observatory, 117, 224
King, J. R., & Hiltgen, D. D. 1996, AJ, 112, 2650
Kraft, R. P. 1965, ApJ, 142, 681
Kurucz, R., & Bell, B. 1995, Kurucz CD-ROM 23, Atomic Line Data (Cambridge: SAO)
Kurucz, R. L., Furenlid, I., & Brault, J. 1984, Solar Flux Atlas from 296 to 1300 nm (Sunspot: National Solar Obs.)
Laughlin, G., & Adams, F. C. 1997, ApJ, 491, L51
Laws, C., & Gonzalez, G. 2001, ApJ, 553, 405
Murray, N., & Chaboyer, B. 2002, ApJ, 566, 442
Patience, J., Ghez, A. M., Reid, I. N., Weinberger, A. J., & Matthews, K. 1998, AJ, 115, 1972
Paulson, D. B., Saar, S. H., & Cochran, W. D. 2003, AJ, submitted
Paulson, D. B., Saar, S. H., Cochran, W. D., & Hatzes, A. P. 2002, AJ, 124, 572 (Pa02)
Perryman, M. A. C., et al. 1998, A&A, 331, 81 (Pe98)
Pinsonneault, M. H., DePoy, D. L., & Coffee, M. 2001, ApJ, 556, L59
Prochaska, J. X., Naumov, S. O., Carney, B. W., McWilliam, A., & Wolfe, A. M. 2000, AJ, 120, 2513
Saar, S., & Osten, R. 1997, MNRAS, 284, 803
Smith, V. V., Cunha, K., & Lazzaro, D. 2001, AJ, 121, 3207
Sneden, C. A. 1973, Ph.D. thesis, Univ. of Texas
Takeda, Y., Kawanomoto, S., Takada-Hidai, M., & Sadakane, K. 1998, PASJ, 50, 509
Takeda, Y., & Sadakane, K. 1997, PASJ, 49, 367
Unsöld, A. 1955, Physik der Sternatmospharen, mit besonderer Berucksichtigung der Sonne (Berlin: Springer)
Varenne, O., & Monier, R. 1999, A&A, 351, 247
Vogt, S. S., et al. 1994, Proc. Soc. Photo-opt. Instrum. Eng., 2198, 362

The Astronomical Journal, 130:2436, 2005 November

ERRATUM: "SEARCHING FOR PLANETS IN THE HYADES. IV. DIFFERENTIAL ABUNDANCE ANALYSIS OF HYADES DWARFS" (AJ, 125, 3185 [2003])

Diane B. Paulson and Christopher Sneden
Department of Astronomy, University of Texas

and

William D. Cochran
McDonald Observatory, University of Texas

In the bottom panel of Figure 5, the data from R. P. Kraft (ApJ, 142, 681 [1965]) (*open squares*) were incorrectly plotted. The corrected figure is included in this erratum. Because the fits shown in both the top and bottom panels of Figure 5 were to our data alone and not to the Kraft data, the adjustment of these data points does not affect the results of this paper. However, we direct the reader to D. R. Soderblom et al. (ApJS, 85, 315 [1993]) for a more in-depth analysis of the rotational velocity of the higher mass objects in the Hyades. We wish to thank D. Soderblom for pointing out this error to us.

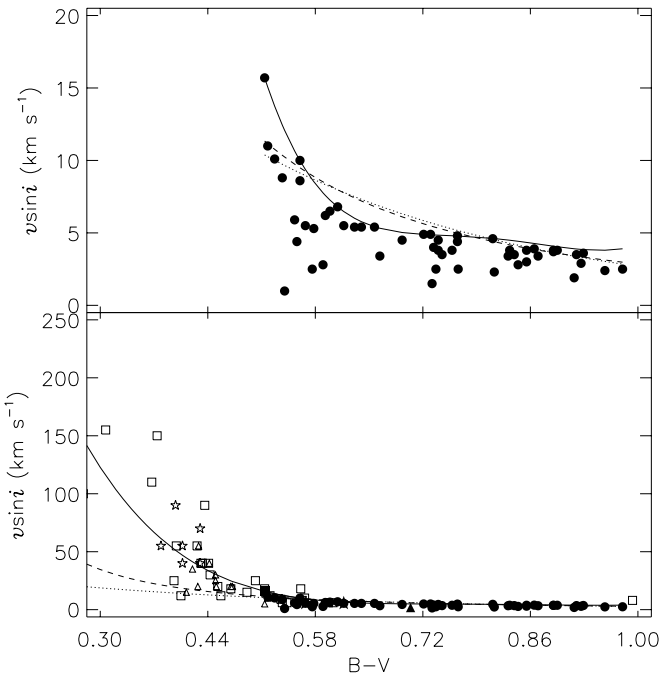

Fig. 5.—Plot of $v \sin i$ of observed Hyades stars (including the same possible nonmembers, as discussed in Fig. 3). The symbols are the same as in Fig. 3. The solid curve is a polynomial fit to the upper envelope of our data (*filled circles*) as discussed in the text, the dashed curve is a power-law fit to our data only, and the dotted curve is an exponential fit to our data, as well. The top panel shows only our data, while the bottom panel adds in $v \sin i$ measurements from E. Böhm-Vitense et al. (ApJ, 569, 941 [2002]) (*open triangles*), W. Benz et al. (A&A, 138, 93 [1984]) (*open stars*), and selected dwarfs from R. P. Kraft (ApJ, 142, 681 [1965]) (*open squares*).